DNA polymorphism sensitive impedimetric detection on gold-nanoislands-modified electrodes

Alessandra Bonanni[1,*], Maria Isabel Pividori[2], Manel del Valle[2,*]

[1] *Division of Chemistry & Biological Chemistry, School of Physical and Mathematical Sciences, Nanyang Technological University, Singapore 63737, Singapore*

[2] *Sensors and Biosensors Group, Department of Chemistry, Universitat Autònoma de Barcelona, Edifici Cn, 08193 Bellaterra, Barcelona, SPAIN*

Abstract

Nanocomposite materials are being increasingly being used in biosensing applications as they can significantly improve biosensor performances. Here we report the use of a novel imedimetric genosensor based on gold nanoparticles graphite-epoxy nanocomposite (nanoAu-GEC) for the detection of triple base mutation deletion in a cystic-fibrosis (CF) related human DNA sequence. The developed platform consists of chemisorbing gold nano-islands surrounded by rigid, non-chemisorbing, and conducting graphite-epoxy composite. The ratio of the gold nanoparticles in the composite was carefully optimized by electrochemical and microscopy studies.

Such platform allows the very fast and stable immobilization of DNA probes on the gold islands, thus minimizing the steric and electrostatic repulsion among the DNA probes and improving the detection of DNA polymorphism up to 2.25 fmol by using electrochemical impedance spectroscopy. These findings are very important in order to develop new and renewable platforms to be used in point-of-care devices for the detection of biomolecules.

Keywords: gold nanocomposite, DNA polymorphism, electrochemical impedance spectroscopy, cyctic fibrosis, gold nanoparticles amplification.

* E-mail: a.bonanni@ntu.edu.sg; Tel.: +65 63168757; Fax: +65 6791 1961 (A.Bonanni)

* E-mail: manel.delvalle@uab.cat; Tel: +34 93 5811017; Fax: +34 93 5812477 (M.del Valle)

1. Introduction

There is a great demand for new materials and protocols for developing novel analytical devices to be employed in the sensitive and specific detection of DNA sequences [1-5]. DNA biosensors (or genosensors) are devices that combine DNA strands as biorecognition element and a transducer that converts the biorecognition event into a measurable analytical signal [6]. To represent a valid alternative to classical techniques for DNA analysis, a genosensor should possess specific features like simplicity, portability, low cost and fast response, and this is normally accomplished with electrochemical transduction. So far, the most used electrochemical transducers for DNA immobilization and detection have been mainly based on gold [4, 7] and carbon materials [3, 8-10]. On the one hand, gold present the advantage of the simple protocols involved in the DNA immobilization; these are based on the strong affinity of thiols to metal surfaces, by using the well-known sulphur chemistry. It should be pointed out that the standard way for thiolating a strand of DNA is to attach a $HS(CH_2)_6$– linker molecule to the end of a phosphate group. In continuous gold surfaces, van der Waals attraction drives the assembly and ordering of DNA probes in typical self-assembled monolayers (SAMs) [11, 12]. However, in such configuration the immobilized DNA probes are subject to strong electrostatic repulsion. As a result, tightly packed and negatively charged SAM are obtained, which could impede the hybridization with the cDNA probe due to both steric as well as electrostatic effects [13], and thus reducing the analytical performance of the genosensors.

On the other hand, carbon presents the advantage of being an inexpensive platform with excellent electrical properties, such as a wide range of working potentials, low electrical resistance, and low residual currents [14-16]. Furthermore, carbon is an ideal choice as composite filler due to its high chemical inertness.

The combination of the feasibility of gold with the versatility of carbon has been recently proposed in few works for the improvement of genosensor performances [17, 18]. The use of gold nanoparticles in a graphite-epoxy composite (nano-AuGEC) was recently reported by our laboratory [19] in order to avoid the stringent control of surface coverage parameters during immobilization of thiolated oligonucleotides. The developed nano-AuGEC brings out islands of chemisorbing material (gold nanoparticles) surrounded by rigid, non-chemisorbing, and conducting graphite-epoxy composite. With this arrangement in the electrochemical transducer, the resulting less-packed surface provided improved hybridization features with a complementary probe by minimizing steric and electrostatic repulsion. Moreover, this platform could be easily renewed for further uses by simple polishing procedure due to the gold integration into the rigid graphite-epoxy composite.

In this work, gold nanoparticles in a graphite-epoxy nanocomposite were employed for the impedimetric detection of DNA sequences. Electrochemical impedance spectroscopy (EIS) was used for the first time both for the characterization of the platform and for DNA polymorphism detection correlated to the development of cystic fibrosis [20, 21]. EIS is a very sensitive technique used for probing the interfacial properties of modified electrodes [22, 23]. However, when dealing with impedance it is very important to work with a reproducible and stable platform, in order to avoid any non-specific interaction that could generate a non-reliable signal [24]. Such a platform was obtained here by immobilizing DNA probes on the chemisorbing gold islands of the composite surface surrounded by rigid, non-chemisorbing and conducting graphite-epoxy composite by simple and fast sulphur chemistry, as shown in Scheme 1.

The microscopic and electrochemical characterization of this material is presented in this paper, as well as the application of the biosensor for the impedimetric genosensing of DNA polymorphism correlated to the development of cystic fibrosis.

2. Experimental

2.1 Materials

Single-stranded DNA oligonucleotides (ssDNA) used in the study were prepared by TIB-MOLBIOL (Berlin, Germany). Their sequences and modifications are listed in Table 1. The target oligonucleotide corresponds to triple base deletion (ΔF508) in a cystic fibrosis (CF) related human DNA sequence (NCBI Reference Sequence: NM_000492.2). The sequence with triple deletion (mutant), which is the analyte sought for diagnosing the genetically inherited illness, was chosen as complementary target. The wild-type corresponds to the gene belonging to healthy individuals. Oligonucleotide stock solutions were diluted with Milli-Q water (18.2 MΩ·cm resistivity), separated in fractions and stored at a temperature of -20°C until used.

Potassium ferricyanide $K_3[Fe(CN)_6]$, potassium ferrocyanide $K_4[Fe(CN)_6]$ and poly(etheyleneglycol) (PEG) were purchased from Sigma-Aldrich (St. Louis, MI). Streptavidin-gold nanoparticles (EM.STP20) were supplied by British BioCell International (BBI, Cardiff, UK). Quantum dots Qdot 655 streptavidin conjugate (Q10121MP, excitation λ 425 nm, emission λ 655 nm) were supplied by Invitrogen (Carlsbad, CA). Other reagents were commercially available and were all of analytical reagent grade. All solutions were made up using doubly distilled water.

The following buffer solutions were employed: PBS1 (0.1 M NaCl, 0.01 M sodium phosphate buffer, pH 7.0), PBS2 (0.01M sodium phosphate buffer, pH 7.0), TSC1 (0.75 M NaCl, 0.075 M trisodium citrate, pH 7.0), TSC2 (0.30 M NaCl, 0.030 M trisodium citrate, pH 7.0).

NanoAu-GEC electrodes were prepared using 50-µm particle size graphite powder (BDH laboratory Supplies, UK), Epotek H77 resin and hardener (both from Epoxy Technology, USA) and gold nanoparticles (nanopowder, <100 nm particle size, product no. 636347 from Aldrich, St. Louis, MI).

2.2 Methods

2.2.1 NanoAu-GEC electrode assembly

Graphite powder and epoxy resin in a 1:4 (w/w) ratio were thoroughly hand mixed to ensure the uniform dispersion of the graphite powder throughout the polymer. For the nanoAu-GEC electrodes, the following ratios of gold nanoparticles, graphite powder, and epoxy resin were prepared: 0.075:0.925:4 (w/w) for nanoAu(7.5%)-GEC; 0.250:0.750:4 (w/w) for nanoAu(25%)-GEC [19]. The electrode consisted of a PVC tube body (6 mm i.d.) and a small copper disk soldered at the end of an electrical connector [25]. The prepared composite was deposited by filling the 3 mm cavity in the PVC body. After filling the electrode body gap completely with the soft paste, the electrode was tightly packed. The composite material was cured at 80°C during 1 week. Before each use, the surface electrode was wetted with doubly-distilled water; it was then thoroughly smoothed with abrasive paper and finally with alumina paper (polishing strips 301044-001, Orion).

2.2.2 Electrochemical characterization of bare nanoAu-GEC electrodes

Cyclic voltammetry and impedance measurements for nanoAu(0%)-GEC (control GEC electrode), nanoAu(7.5%)-GEC and nanoAu(25%)-GEC bare electrodes were performed. Both kind of measurements were carried out in PBS1 buffer, pH 7.0, containing 10 mM $K_3[Fe(CN)_6]/K_4[Fe(CN)_6]$ (1:1) mixture, used as a redox probe.

An IM6e Impedance Measurement Unit (BAS-Zahner, Germany) was employed for all electrochemical measurements. Thales software was used for the acquisition of the data and the control of the experiments. A three electrode cell was used to perform the impedance measurements: it was formed by an Ag/AgCl reference electrode, i.e. an AgCl covered silver wire, a ring-platinum electrode (Crison 52-67-1, Barcelona, Spain) and the assembled nanoAu-GEC working electrode.

Cyclic voltammetry was carried out between -0.75 and +1.25 V (vs Ag/AgCl) at 100 mV s^{-1} scan rate in a 20 mL electrochemical cell at room temperature [19].

Impedance spectra were recorded between 50 KHz-0.05 Hz, at 10 mV amplitude and at a sampling rate of 10 points per decade above 66 Hz and 5 points per decade at the lower range. The experiments were carried out under open circuit potential conditions. The obtained spectra were represented as Nyquist plots ($-Z_i$ vs. Z_r) in the complex plane. A Randles equivalent circuit was used to fit the impedance data. The chi-square goodness of fit was calculated for each fitting by the FRA software employed (Eco Chemie, the Netherlands).

2.2.3 Microscopic characterization of nanoAu-GEC bare electrode surface

A Scanning Electron Microscope (SEM) (Hitachi S-570, Tokyo, Japan) and a Leica MZ FLIII fluorescence stereomicroscope (Leica, Heidelberg, Germany) were used to study the distribution of the gold nanoparticles on the electrode surface. A LEICA TCS SP2 AOBS microscope was used to take confocal laser scanning microphotographs of the electrodes (laser excitation: 568 nm; voltage: 352 V).

Microscopy characterization of the nanoAu(7.5%)-GEC (optimized platform) was performed. SEM images of GEC and nanoAu(7.5%)-GEC surface were taken at acceleration voltage of 20 kV and resolution of 100 μm. Fluorescence microscopy images of GEC and nanoAu(7.5%)-GEC modified with SH-probe-fluorescein oligo were also taken. The immobilization of the latter was performed in TSC1 buffer with 200 pmol of double-tagged oligomer at a final volume of 140 μL for 2 h at 42°C under gentle stirring. Two washing steps were then performed with 140 μL TSC2 buffer, for 10 min at 42°C under gentle stirring.

2.2.4 Immobilization of DNA probe on nanoAu-GEC electrode surface

The immobilization was achieved by incubating the nanoAu-GEC electrode in an Eppendorf tube with 140 μL of the SH-probe solution at desired concentration in TSC1 buffer, for 30 min at 42°C. This was followed by two gentle washing steps with TSC2 buffer for 10 min at 42°C, in order to remove non-specific adsorbed probe oligonucleotides. Before hybridization, a blocking step was performed in order to avoid non-specific adsorption of target oligonucleotides. For this purpose, the electrode surface was treated with a 0.02 mM solution of PEG [26] in PBS1, pH=7, for 15 min and then rinsed with PBS1.

2.2.5 Hybridization with DNA target

NanoAu-GEC electrodes modified with SH-probe were incubated in an Eppendorf tube with the hybridization solution containing the DNA target in TSC1 buffer. The total volume of the solution in each tube was 140 μL and the incubation was performed at 42ºC during 30 minutes, with gentle stirring. Two washing steps were then performed in TSC2 buffer at 42ºC for 10 minutes. Three different DNA sequences were used in this step: a fully complementary sequence (mutant), a three bases insertion sequence (wild-type), a non-complementary sequence (nc).

2.2.6 Addition of streptavidin-modified gold nanoparticles (strept-AuNPs)

In this step the signaling probe and the strept-AuNPs (1/100 dilution from stock solution) were previously incubated in PBS2 buffer, pH=7, during 30 min. After that, nanoAu-GEC electrodes modified with DNA hybrid were incubated in signaling probe/strept-AuNP conjugate solution for 30 min at 42°C under gentle stirring. Two washing steps were then performed in TSC2 buffer at 42ºC for 10 minutes.

In all cases impedance data were recorded in the following order after each step: (1) bare electrode (blank); (2) probe immobilization; (3) hybridization with target; (4) hybridization with signaling probe previously conjugated with strept-AuNPs. The whole protocol is represented in Scheme 1.

3. Results and discussion

The proposed research combines the easy assembling of the GEC electrodes with the straightforward immobilization of biological component on gold nanoparticles in a novel nanocomposite transducer for impedimetric genosensing. The idea was to generate gold islands into the epoxy-graphite surface, in order to provide anchoring points for immobilizing DNA probes through gold-sulphur chemistry. For further evaluation of the nanoAu-GEC electrodes, the characterization of the surface was performed both by electrochemistry and by electron microscopy. Moreover, the optimization of biosensing protocol was performed through electrochemical evaluation and fluorescence visualization of the effects of DNA probe and target concentration on the electrode surface.

Both voltammetric and impedimetric results showed that nanoAu(0%)-GEC and nanoAu(7.5%)-GEC present similar electrochemical behavior. As shown in Figure S1 part A (see Supporting Information), a very similar CV profile for ferrocyanide/ferricyanide redox probe was obtained for both nanoAu(0%)-GEC and nanoAu(7.5%)-GEC. When increasing the amount of gold nanoparticles (nanoAu(25%)-GEC), the peak separation increased, showing a slower electron transfer rate on that material. This effect, which has been previously reported [19], is attributable to an increasing amount of gold aggregates which strongly influences the electrical properties of the composite.

Analogous results were obtained in the impedimetric study, as it could be expected. In fact, as shown in Figure S1, part B, the Nyquist plots obtained in presence of the redox probe indicated a similar and faster charge transfer rate for nanoAu(0%)-GEC and nanoAu(7.5%)-GEC electrodes, which present comparably low charge transfer resistance values. On the other hand, Nyquist plot for nanoAu(25%)-GEC shows an increased charge transfer resistance value, which is consistent with the less ideal electrochemical signal observed in the cyclic voltammetry studies [27, 28]. Moreover, the reproducibility of results obtained with nanoAu(25%)-GEC electrode, either for cyclic voltammetry or for impedance was considerably lower than that obtained for nanoAu(7.5%)-GEC. For all these reasons nanoAu(7.5%)-GEC electrode was chosen as working electrode for the impedimetric genosensing, as also previously reported for amperometric genosensing [19].

The distribution of gold nanoparticles on the electrode surface was studied by scanning electron microscopy. Figure 1B shows, as bright spots, the aggregates of gold nanoparticles for nanoAu(7.5%)-GEC, which resulted well-dispersed within the graphite-epoxy matrix.

Furthermore, the availability of gold nanoparticles in the composite for the immobilization of thiolated oligomers was also studied by fluorescence stereomicroscopy. In this case, 200 pmol of double-tagged oligo with both a thiolated 5′-end and a fluorescein 3′-end was immobilized on nanoAu(7.5%)-GEC electrodes. As it can be seen in Figure 2 for nanoAu(7.5%)-GEC, the fluorescence shows a discontinuous pattern as fluorescence dots corresponding to the chemisorbing material surrounded by nonreactive graphite-epoxy composite. Both SEM and fluorescence study images of nanoAu(0%)-GEC electrodes were taken as negative control for comparison purposes. For a more detailed electrochemical and microscopy characterization of this bare nanoAu-GEC electrode with different gold amount please refer to a previous work from the same laboratory [19].

In order to optimize the DNA probe concentration to be used in the protocol, different EIS measurements were carried out with increasing amounts of probe oligonucleotides. The optimized concentration should ensure a full coverage of the electrode surface in order to avoid non-specific adsorption of both the DNA target and strept-AuNPs. Figure 3 shows the variation (Δ_p) of charge transfer resistance between blank (bare electrode) and probe-modified electrode plotted versus DNA probe concentration. The increase of DNA probe concentration was associated with an enhancement of R_{ct} value until a plateau was reached. At this point, the electrode surface can be considered completely covered by the immobilized oligonucleotide and any additional increase of DNA did not result in a further increase of R_{ct} value. From these observations, a DNA probe concentration of 60 pmol (4×10^{-7} mol L^{-1}) was chosen for subsequent experiments.

Figure 4 shows Nyquist plots obtained in a whole biosensing experiment and the Randles equivalent circuit used to fit the experimental data. Briefly, the parameter R_1 corresponds to the resistance of the solution; R_2 (also called R_{ct}) represents the resistance to the charge transfer between the solution and the electrode surface; and CPE (constant phase element) is associated with the capacitance of the double layer. The use of a CPE instead of a capacitor results in better fitting of the experimental data and it is generally due to the non-homogeneous nature of the electrode surface [29, 30].

Among these electrical parameters, we focused on the change of charge transfer resistance (R_{ct}) value recorded after any further step of the biosensing protocol. In fact, the charge transfer process, due to the redox reaction of the couple $K_3[Fe(CN)_6]/K_4[Fe(CN)_6]$ at the applied potential, is strongly influenced by any electrode surface modification. For this reason it is possible to follow the biosensing event by simply monitoring the variation of R_{ct}. In the Nyquist plot, the R_{ct} value corresponds to the diameter of the semicircle.

The time constant of the semicircles was also monitored after any further electrode surface modification, and no significant changes were observed. The related difference of frequencies at the apex of the semicircle was within ± one experimental step of the scanned frequency. In addition, the chi-square goodness-of-fit test was performed for every fitting to validate the calculations. In all cases, the calculated values for each circuit remained in the range of 0.0025–0.4, much lower than the tabulated value for 50 degrees of freedom (67.505 at the 95% confidence level).

Figure 4 shows that the R_{ct} of the bare electrode (filled circles) significantly increased after SH-probe immobilization (empty squares) onto the sensor surface. This is due to the slower kinetic of $[Fe(CN)_6]^{3-/4-}$ electron transfer process occurring at the electrode surface after modification [22]. The negative charges on the phosphate backbone of the immobilized DNA probe repelled the negatively charged redox probe, thus increasing the R_{ct} value. The steric hindrance generated by the formation of the DNA probe film also contributed to the increase of R_{ct}. After hybridization with the complementary DNA target (mutant) a further increase in charge transfer resistance value was observed (filled squares). In fact, the addition of complementary DNA strand (mutant) to form DNA hybrid resulted in the increment of resistance value due to the increased amount of negative charges and to the hindrance caused by the formation of the hybrid.

After the addition of the signaling probe/strept-AuNPs conjugate we could observe extra increment of charge transfer resistance (empty triangles). It should be considered that the addition of signaling probe/strept-AuNP conjugate resulted in a further increment of resistance value due to the increased amount of negative charges because of the polyanionic nature of the signaling probe covering the strept-AuNPs, as depicted in Scheme 1. Moreover, at working pH 7, streptavidin is slightly negatively charged [31] (p*I* is ca. 5) and this also contributed to enhance the resistance as a consequence of the electrostatic repulsion with the redox probe.

In order to estimate the limit of detection achieved with the developed genosensor and to optimize the concentration of DNA target to be used in the different experiments, the impedimetric response was recorded towards DNA target concentration. Figure 6 represents results obtained in the detection of complementary target (mutant – filled squares) 3-mismatches target (wild-type – empty diamonds); non-complementary target (nc – filled circles). The impedimetric response after the hybridization step was recorded for DNA target concentrations from 0.3 fmol (2×10^{-12} mol L^{-1}) to 3 nmol (2×10^{-6} mol L^{-1}). The concentration of DNA probe was kept constant at the optimized value of 60 pmol (4×10^{-7} mol L^{-1}). Results are expressed as the relative R_{ct} variation between the values obtained in the different experiments (i.e. DNA immobilization or hybridization) and the R_{ct} value due to the bare electrode. This relative variation is represented as a ratio of delta increments ($\Delta_{ratio} = \Delta_s/\Delta_p$, see caption of Figure 3). This elaboration is required for the comparison of data from different electrodes and has already been used and extensively explained in previous works [25]. The Δ_s/Δ_p value should be > 1 for the hybridization experiments and close to 1 for negative controls with non-complementary targets ($\Delta_s = \Delta_p$, i.e. no variation of R_{ct} value after hybridization).

As shown in Figure 5, the increase of target concentration led to a higher analytical signal due to the increase of R_{ct}, thus achieving a linear range between 0.3 fmol (2×10^{-12} mol L^{-1}) and 30 pmol (2×10^{-7} mol L^{-1}). After that, a plateau was reached and any further increment of target concentration did not generate any additional change of the signal. The signal change recorded with the 3-mismatches sequence (wild-type – empty diamonds) was lower than that obtained with the complementary sequence (mutant – filled squares), as expected. Moreover, significant changes of R_{ct} were not recorded when employing the non-complementary sequence in the hybridization step, thus confirming that non-specific interactions can be considered negligible. The achieved limit of detection for the mutant DNA was 22.5 fmol (1.5×10^{-10} mol L^{-1}), whilst the differentiation between complementary and 3-mismatches sequence (mutant/wild-type) was detectable at 45 fmol (3.0×10^{-10} mol L^{-1}). Those detection limits were calculated with a signal to noise ratio S/N = 3. The attained values can be considered of interest, given that they were originated in a direct, unlabelled target-probe interaction, characteristic of impedimetric biosensing. Obviously, to achieve the differentiation usable for clinical diagnostics, a parallel assay with use of equivalent DNA sample amount would be the recommended procedure.

In order to enhance the impedimetric response and improve the limit of detection, a further signal amplification step was performed by employing strep-AuNPs.

As previously stated, an increase of R_{ct} value was achieved by incubating the nanoAu(7.5%)-GEC electrode modified with double stranded DNA hybrid in a solution containing the signaling probe conjugated with strept-AuNPs. The reason for this R_{ct} increase is due to the further steric hindrance and negative charge amount introduced onto the electrode surface. In fact, the polyanionic complex formed by negatively charged strept-AuNPs modified on their surface with the signaling probe oligonucleotides contribute to the increase of negative charges on the electrode surface. Table 2 summarize the obtained results, represented as the relative variation of R_{ct} ($\Delta_{ratio}= \Delta_s/\Delta_p$, see caption on Table 2) for different concentrations of DNA target. In the second and third columns, results obtained in hybridization experiments with mutant and wild-type DNA target before strept-AuNP addition are represented. The fourth and fifth columns show results obtained in hybridization experiments with mutant and wild-type DNA targets after amplification step. Finally, in the sixth and seventh column, the net increase of the amplified signal (calculated as the net gain, see caption to Table 2) due to the hybridization with signaling probe/strept-AuNPs conjugate was calculated.

The R_{ct} increase (net values up to 1.65) obtained in presence of the mutant DNA target is more significant than that recorded for the wild-type DNA target (net values between 0.15 and 0.30, its magnitude in the range of the standard deviations). In the experiments with mutant DNA target, the largest net increase of amplified signal corresponded to the optimized DNA target concentrations of 30 pmol (2×10^{-7} mol L^{-1}). For this concentration the signal for mutant DNA resulted 67% amplified (relative value), when compared with results recorded without the use of strept-AuNPs. In comparison, the relative 13% to 17% signal amplification obtained for the 3-mismatches DNA sequence (wild-type) can be considered not significant. After signal amplification, the achieved limit of detection for the mutant DNA was 2.25 fmol (1.5×10^{-11} mol L^{-1}), whilst the differentiation between complementary and 3-mismatches sequence (mutant/wild-type) was detectable down to 12 fmol (8.0×10^{-11} mol L^{-1}).

An additional experiment was carried out in order to confirm and visualize the hybrid formation onto the electrode surface. To this aim the electrode surface already modified with biotinylated double stranded DNA was incubated in a solution containing streptavidin modified Qdots (strept-QD), which show high yield characteristic fluorescence. The characterization of the nanoAu(7.5%)-GEC surface was then obtained by confocal laser scanning microscopy. The images are shown in Fig. 6.

The first image (A) corresponds to the negative control, where a non-complementary target was used during the hybridization step. The second image (B) corresponds to an experiment where the 3-mismatches sequence (wild-type) was employed. The third image (C) represents the experiment with the complementary target (mutant). In all cases the electrode surface modified with the dsDNA was incubated in a solution containing strept-QD. As expected, a clear spotted fluorescence was observed for the electrode modified with the complementary target (C), whilst a much weaker fluorescence was observed in presence of a 3-mismatches sequence or in the case of non-complementary one. Again, this confirms that non-specific interactions on the developed genosensor can be considered not significant.

4. Conclusions

We reported for the first time a gold nanoparticles graphite-epoxy nanocomposite platform for the impedimetric detection of DNA polymorphism by hybridization. The platform was first carefully characterized both by electrochemical techniques and by microscopy studies. The spatial resolution of gold nanoparticles was demonstrated to be easily controlled by merely varying its percentage in the composite composition. Beside the immobilization capabilities towards thiolated DNA, this novel material shows excellent electrochemical properties similar to those of graphite epoxy composite.

The chemisorbing ability of gold nanoparticles in the nano-AuGEC was demonstrated with an excellent LOD (22.5 fmol of ssDNA target) in label-free hybridization studies with impedimetric detection without the need for complex surface treatment or auxiliary reagents. The limit of detection was additionally improved by a signal amplification step by providing a further increment of resistance due to the increased amount of negative charges because of the polyanionic nature of the signaling probe covering gold nanoparticles.

The nanoAu-GEC material showed interesting properties for impedimetric genosensing in hybridization experiments and very promising features for impedimetric biosensing of a wide range of biomolecules, such as dsDNA, PCR products, affinity proteins, antibodies, or enzymes. Instead of forming SAMs on continuous layers of gold, isolated gold nanoparticles are able to produce bioactive chemisorbing islands for the immobilization of thiolated biomolecules, avoiding stringent conditions for surface preparation as well as the use of auxiliary reagents such as lateral spacer thiols. Less compact layers are thus achieved favoring the recognition event on biosensing devices. As such, hybridization efficiency is expected to be higher on the edges of the gold nanoparticles surrounded by nonreactive graphite−epoxy composite. The EIS technique demonstrated again a remarkable versatility for biosensing, as it can be used for characterization, but also for transduction. Moreover it allows performing the latter either in label-free mode, or by using signaling or amplification stages.

To conclude, rigid conducting gold nanocomposite represents a good material for the improved and oriented immobilization of biomolecules with excellent transducing properties for the construction of a wide range of impedimetric biosensors such as immunosensors, genosensors, and enzymatic sensors.

Acknowledgements

Financial support for this work has been provided by the Ministry of Science and Technology (MCyT, Madrid, Spain) through projects CTQ2010-17099, BIO2010-17566 and the program ICREA Academia.

References

[1] A. Erdem, Talanta, 74 (2007) 318-325.
[2] C. Dhand, M. Das, M. Datta, B.D. Malhotra, Biosens. Bioelectron., 26 (2011) 2811-2821.
[3] S.K. Vashist, D. Zheng, K. Al-Rubeaan, J.H.T. Luong, F.S. Sheu, Biotechnology Advances, 29 (2011) 169-188.
[4] M. Vidotti, R.F. Carvalhal, R.K. Mendes, D.C.M. Ferreira, L.T. Kubota, J. Braz. Chem. Soc., 22 (2011) 3-20.
[5] J.B. Haun, T.J. Yoon, H. Lee, R. Weissleder, Wiley Interdisciplinary Reviews-Nanomedicine and Nanobiotechnology, 2 (2010) 291-304.
[6] R.W. Cattrall, Chemical Sensors, Oxford University Press, Oxford (UK), 1997.
[7] F. Lucarelli, G. Marrazza, A.P.F. Turner, M. Mascini, Biosens. Bioelectron., 19 (2004) 515-530.
[8] C.B. Jacobs, M.J. Peairs, B.J. Venton, Anal. Chim. Acta, 662 (2010) 105-127.
[9] Y.Y. Shao, J. Wang, H. Wu, J. Liu, I.A. Aksay, Y.H. Lin, Electroanalysis, 22 (2010) 1027-1036.
[10] A. Bonanni, A.H. Loo, M. Pumera, TrAC Trends Anal. Chem., 37 (2012) 12-21.
[11] S.K. Arya, P.R. Solanki, M. Datta, B.D. Malhotra, Biosens. Bioelectron., 24 (2009) 2810-2817.
[12] P. Pandey, S.K. Arya, Z. Matharu, S.P. Singh, M. Datta, B.D. Malhotra, J. Appl. Polym. Sci., 110 (2008) 988-994.
[13] E. Huang, M. Satjapipat, S.B. Han, F.M. Zhou, Langmuir, 17 (2001) 1215-1224.
[14] M.I. Pividori, S. Alegret, Anal. Lett., 36 (2003) 1669-1695.
[15] S.H. Zuo, L.F. Zhang, H.H. Yuan, M.B. Lan, G.A. Lawrance, G. Wei, Bioelectrochem., 74 (2009) 223-226.
[16] J. Wang, A.N. Kawde, Anal. Chim. Acta, 431 (2001) 219-224.
[17] S.N. Kim, J.M. Slocik, R.R. Naik, Small, 6 (2010) 1992-1995.
[18] Y.Z. Zhang, H.Y. Ma, K.Y. Zhang, S.J. Zhang, J. Wang, Electrochim. Acta, 54 (2009) 2385-2391.
[19] P. Marques, A. Lermo, S. Campoy, H. Yamanaka, J. Barbe, S. Alegret, M.I. Pividori, Anal. Chem., 81 (2009) 1332-1339.
[20] J.L. Bobadilla, M. Macek, J.P. Fine, P.M. Farrell, Human Mutation, 19 (2002) 575-606.
[21] B.S. Kerem, J.M. Rommens, J.A. Buchanan, D. Markiewicz, T.K. Cox, A. Chakravarti, M. Buchwald, L.C. Tsui, Science, 245 (1989) 1073-1080.
[22] E. Katz, I. Willner, Electroanalysis, 15 (2003) 913-947.
[23] A. Bonanni, M. del Valle, Anal. Chim. Acta, 678 (2010) 7-17.
[24] A. Bogomolova, E. Komarova, K. Reber, T. Gerasimov, O. Yavuz, S. Bhatt, M. Aldissi, Anal. Chem., 81 (2009) 3944-3949.
[25] A. Bonanni, M.J. Esplandiu, M.I. Pividori, S. Alegret, M. del Valle, Anal. Bioanal. Chem., 385 (2006) 1195-1201.
[26] T.H.M. Kjallman, H. Peng, C. Soeller, J. Travas-Sejdic, Anal. Chem., 80 (2008) 9460-9466.
[27] A. Bonanni, M. Pumera, Y. Miyahara, Phys. Chem. Chem. Phys., 13 (2011) 4980-4986.
[28] S.W. Chen, Anal. Chim. Acta, 496 (2003) 29-37.
[29] C. Gabrielli, Use and Application of Electrochemical Impedance Techniques, Solartron Analytical, Farnborough, UK, 1990.
[30] J.R. Macdonald, Impedance Spectroscopy, Wiley, New York, 1987.
[31] S. Sivasankar, S. Subramaniam, D. Leckband, Proceedings of the National Academy of Sciences of the United States of America, 95 (1998) 12961-12966.

FIGURE CAPTIONS

Scheme 1. Schematic of the experimental protocol for SH-probe immobilization (step 1), followed by hybridization (step 2) and signal amplification (step 3).

Figure 1 . Scanning electron microscopy images of (A): nanoAu(0%)-GEC and (B): nanoAu(7.5%)-GEC surface. All images were taken at acceleration voltage of 20 kV and resolution of 100µm.

Figure 2. Fluorecence stereomicroscopy at low resolution showing the fluorescence pattern of (A): nanoAu(0%)-GEC and (B): nanoAu(7.5%)-GEC surface after the immobilization of 200 pmol of double tagged oligo with thiol and fluorescein ends**.**

Figure 3. Curve representing experiments for optimization of the ssDNA probe concentration ($\Delta_p = R_{ct(probe)} - R_{ct(blank)}$). Error bars correspond to standard deviation (n=3).

Figure 4. Nyquist plots, $-Z_i$ vs. Z_r, of: bare nanoAu(7.5%)-GEC electrode (black diamonds); SH-probe modified nanoAu(7.5%)-GEC (blue squares); hybrid modified nanoAu(7.5%)-GEC (red triangles); hybrid + AuNPs modified nanoAu(7.5%)-GEC (filled circles). Concentration of DNA probe: 60 pmol (4×10^{-7} M); concentration of DNA target: 30 pmol (2×10^{-7} M). All measurements were performed in 0.1M PBS buffer solution containing 10 mM $K_3[Fe(CN)_6]/K_4[Fe(CN)_6]$. Randles equivalent circuit used for data fitting is included in the figure.

Figure 5. Curves representing impedimetric response towards DNA target concentration in the case of: complementary target (mutant – filled squares); 3-mismatches target (wild-type – empty diamonds); non-complementary target (negative control – filled circles)**.** $\Delta_{ratio} = \Delta_s/\Delta_p$; $\Delta_s = R_{ct\ (sample)} - R_{ct\ (blank)}$; $\Delta_p = R_{ct\ (probe)} - R_{ct\ (blank)}$). Error bars correspond to standard deviation (n=3).

Figure 6. Images obtained with a confocal laser scanning microscope, using strept-QDs modified signaling probes, in experiments with: (A) non-complementary target (negative control); (B) 3-mismatches target (wild-type); (C) complementary target (mutant). Strept-QD final concentration: 10 nM. Laser excitation: 425 nm. Voltage: 352 V. Images were taken by integrating the fluorescence in five different planes in which signal was detected.

Table 1. Summary of DNA oligomers used in this work

Name	Sequence	Modification
SH-probe	GAAACACCAA TGATATTTTC	5'-SH
SH-probe-FL	CGCTCAATGC CTGGAGAT	5'-SH 3'-fluorescein
mutant	TTTTCCTGGA TTATGCCTGG CACCATTAAA GAAAATATCA TTGGTGTTTC	-
wild-type	TTTTCCTGGA TTATGCCTGG CACCATTAAA GAAAATATCA T<u>**CTT**</u>TGGTGT TTC	-
non-complementary (nc)	TTTTTTTTTT TTTTTTTTTT TTTTTTTTTT TTTTTTTTTT TTTTTTTTTT	-
signaling probe	CCAGGCATAA TCCAGGAAAA	5'-biotin

Table 2. Impedimetric response towards DNA target concentration before and after AuNP addition†

DNA target concentration (mol L^{-1})	Δ_{ratio} before strept-AuNPs *		Δ_{ratio} after strept-AuNPs **		Net signal gain ***	
	mutant	wild-type	mutant	wild-type	mutant	wild-type
2×10^{-12}	1.30 (0.10)	1.10 (0.12)	1.80 (0.21)	1.25 (0.13)	0.50	0.15
2×10^{-11}	1.51 (0.11)	1.31 (0.09)	2.21 (0.19)	1.49 (0.22)	0.70	0.18
2×10^{-10}	1.82 (0.09)	1.45 (0.09)	2.62 (0.20)	1.65 (0.20)	0.80	0.20
2×10^{-9}	2.01 (0.12)	1.56 (0.11)	3.12 (0.16)	1.75 (0.15)	1.11	0.19
2×10^{-8}	2.33 (0.10)	1.71 (0.10)	3.64 (0.18)	1.96 (0.20)	1.31	0.25
2×10^{-7}	2.45 (0.15)	1.73 (0.15)	4.10 (0.18)	2.03 (0.20)	1.65	0.30
2×10^{-6}	2.50 (0.13)	1.75 (0.14)	4.09 (0.20)	2.04 (0.23)	1.59	0.29

†Values in parentheses represent the standard deviations (n≥3).

*Δ_{ratio} before strept-AuNPs = Δ_s/Δ_p;
$\Delta_s = R_{ct\ (sample)} - R_{ct\ (blank)}$; $\Delta_p = R_{ct\ (probe)} - R_{ct\ (blank)}$; Sample = dsDNA

**Δ_{ratio} after strept-AuNPs = Δ_s/Δ_p;
$\Delta_s = R_{ct\ (sample)} – R_{ct\ (blank)}$; $\Delta_p = R_{ct\ (probe)} – R_{ct\ (blank)}$. Sample = dsDNA+ strept-AuNPs

***Net signal gain, Δ_{ratio} after strept-AuNPs – Δ_{ratio} before strept-AuNPs

Scheme 1

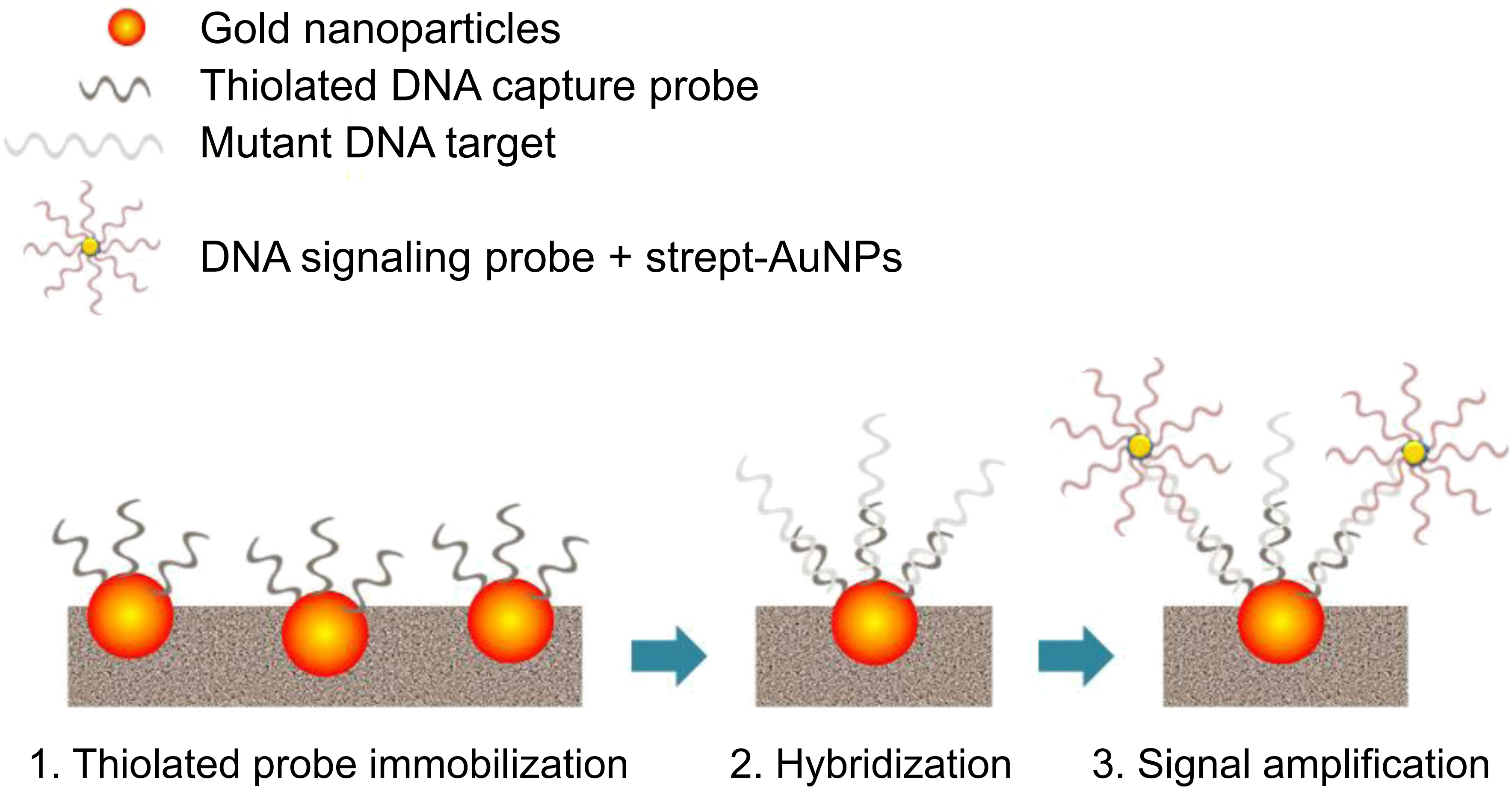

Gold nanoparticles
Thiolated DNA capture probe
Mutant DNA target
DNA signaling probe + strept-AuNPs
1. Thiolated probe immobilization
2. Hybridization
3. Signal amplification

Figure 1

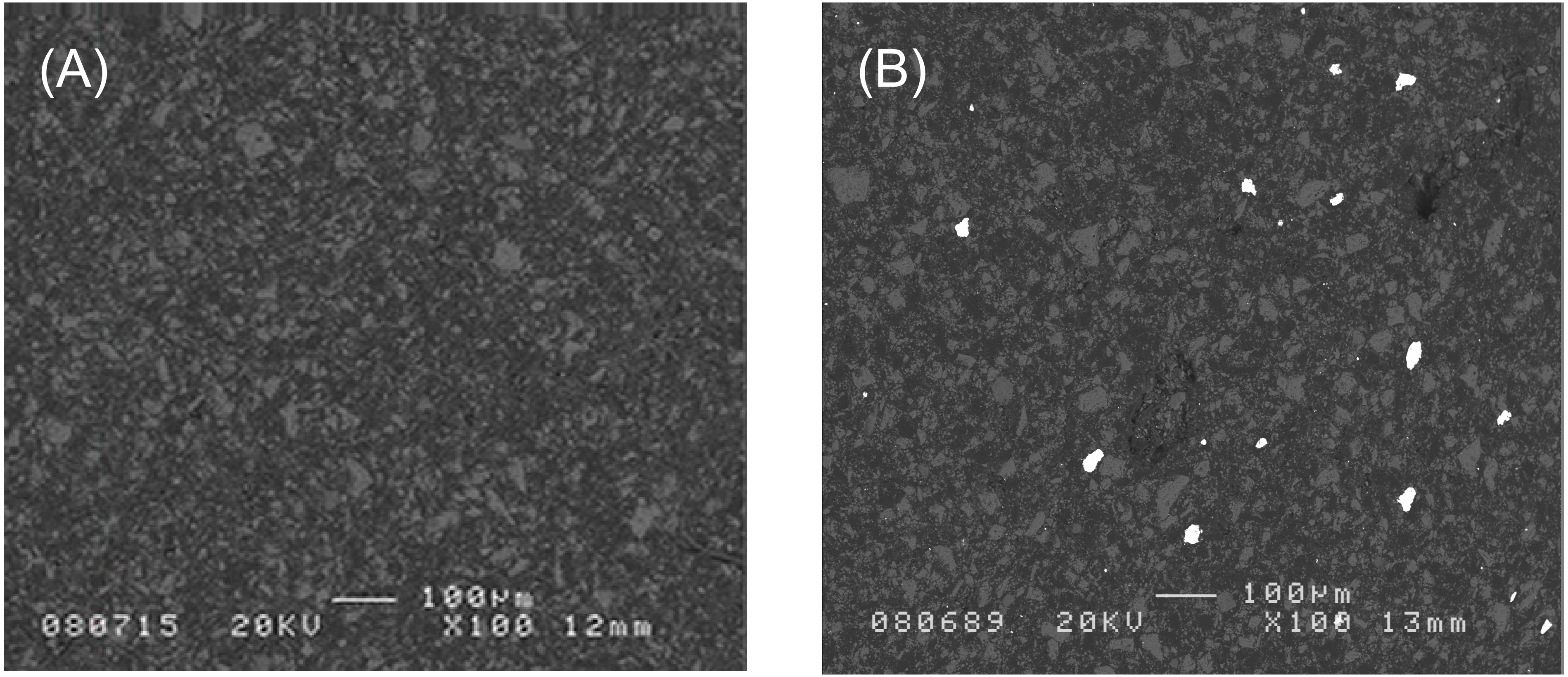

Figure 2

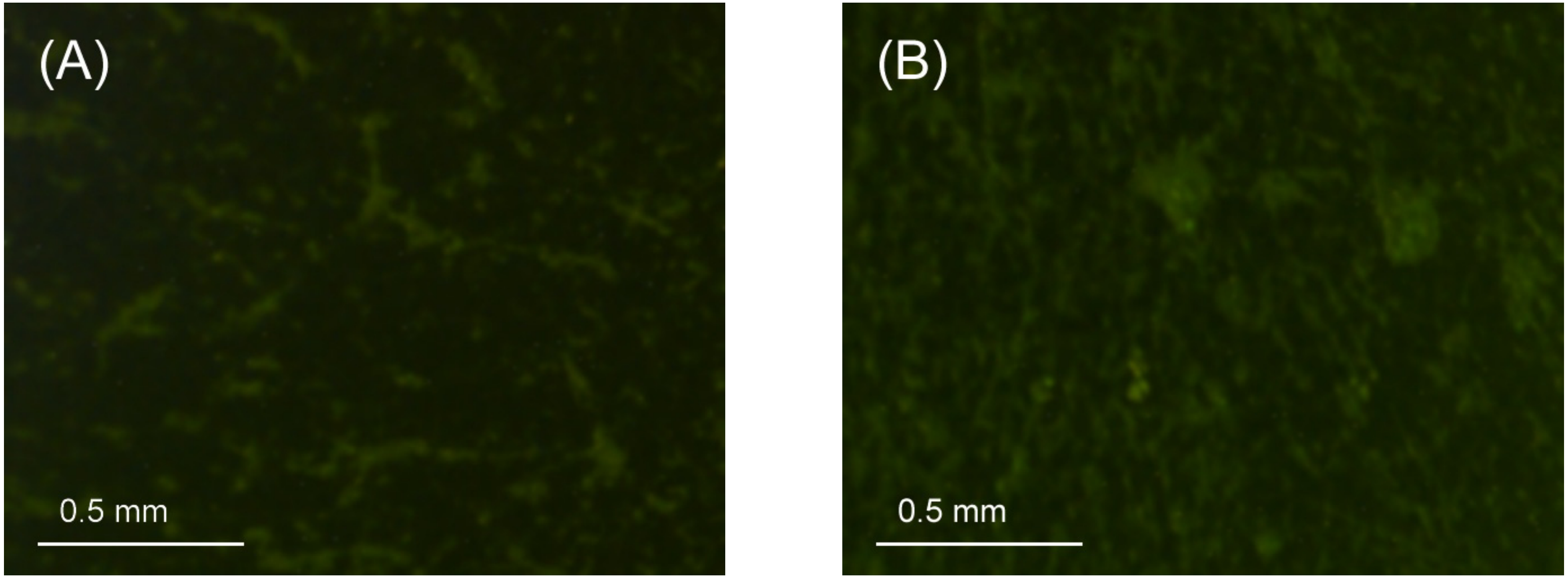

Figure 3

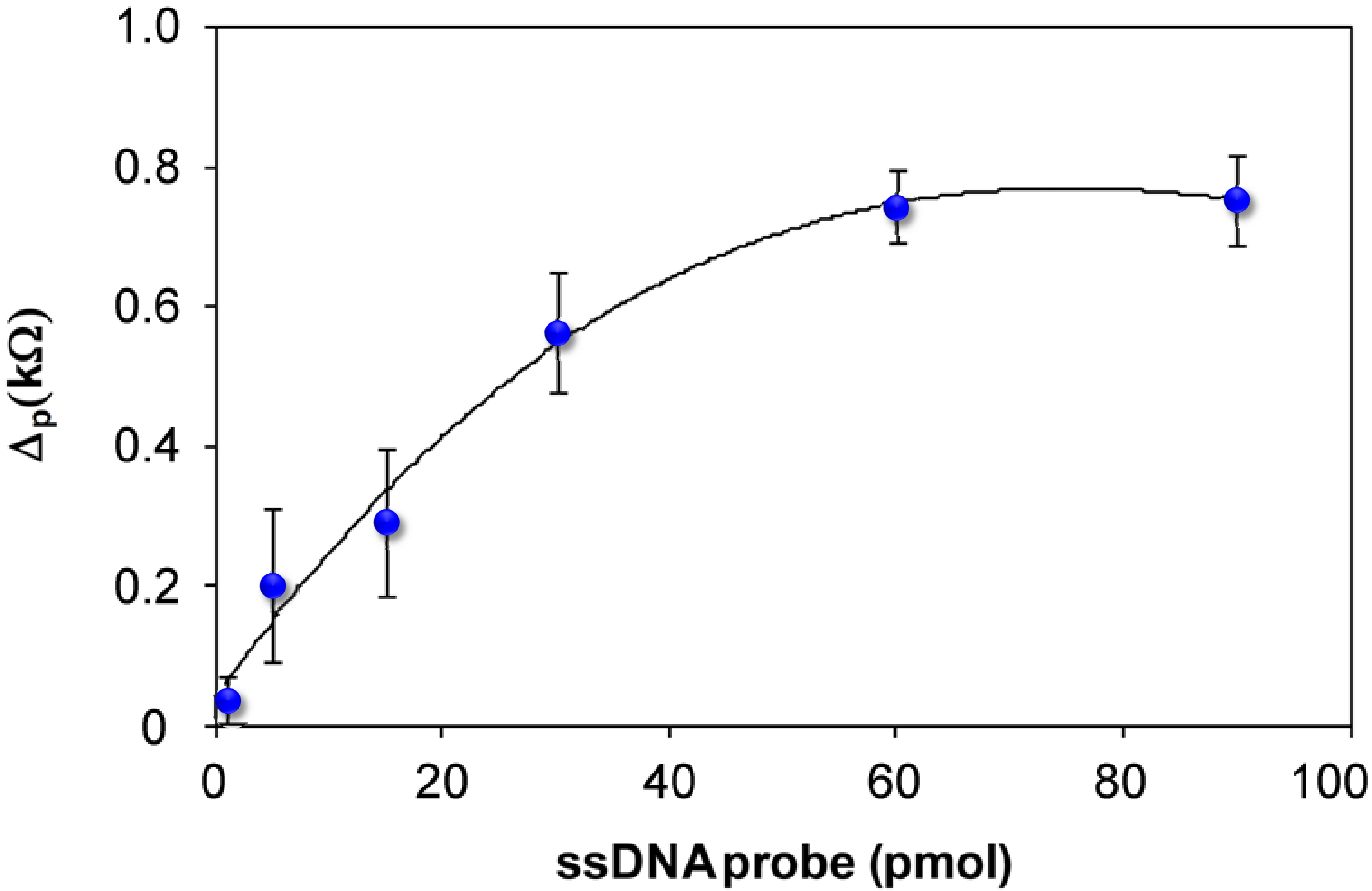

Figure 4

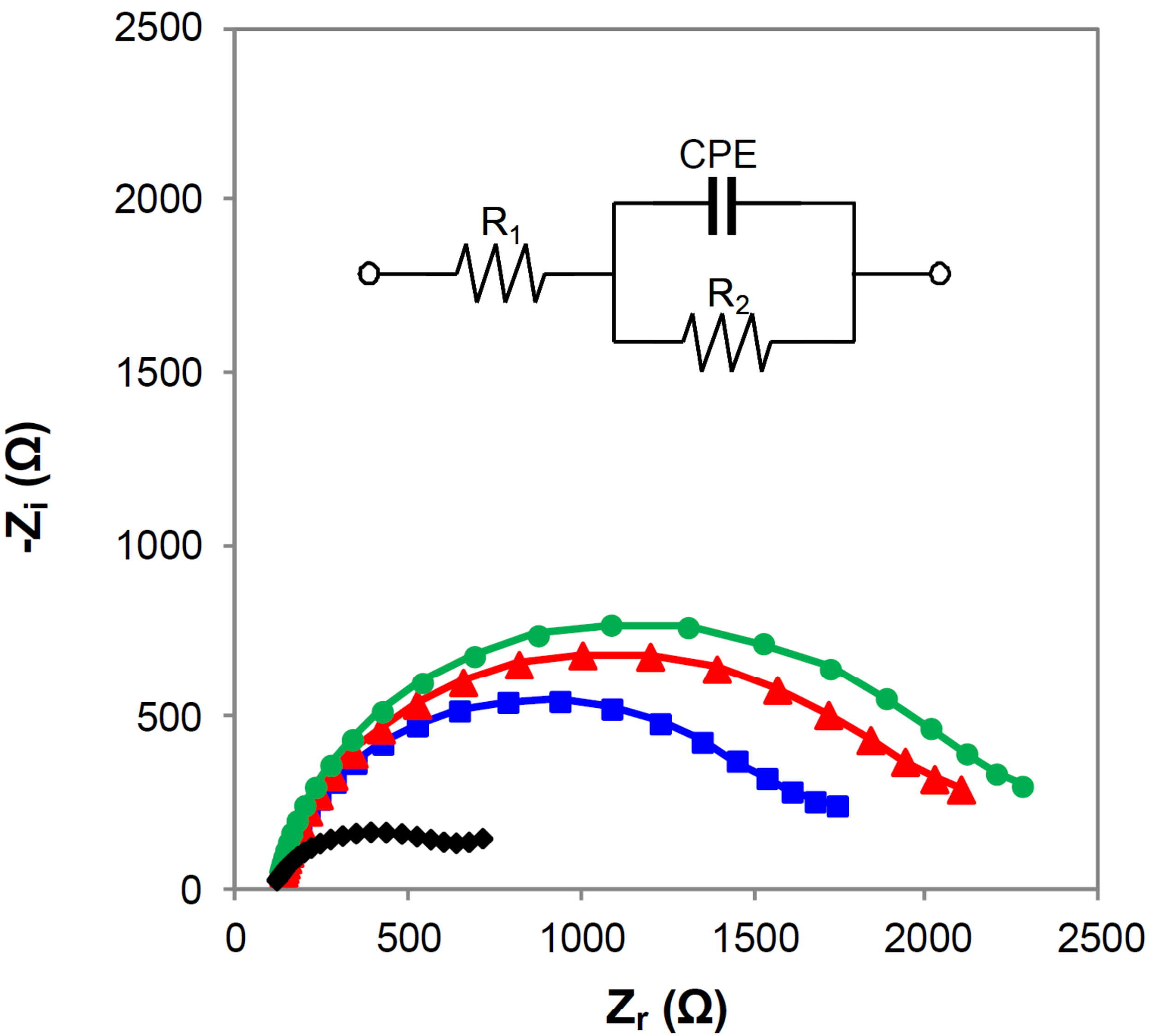

CPE
R1
R2
2500
2000
1500
1000
500
0
0
500
1000
1500
2000
2500
-Zi (Ω)
Zr (Ω)

Figure 5

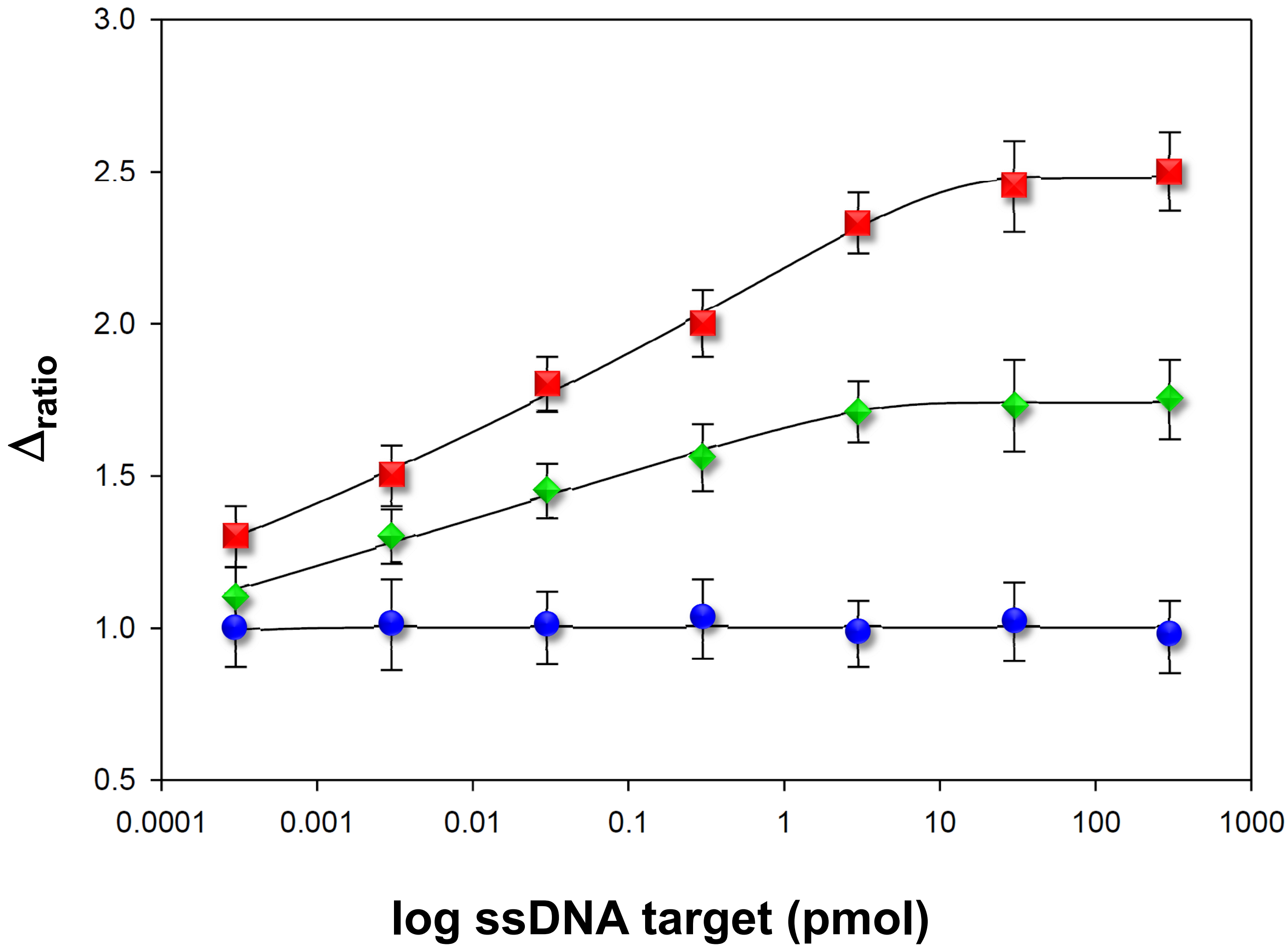

3.0
2.5
2.0
1.5
1.0
0.5
Δ_{ratio}
0.0001
0.001
0.01
0.1
1
10
100
1000
log ssDNA target (pmol)

Figure 6